MOLECULAR ECOLOGY

Molecular Ecology (2014) **23**, 1544–1557 doi: 10.1111/mec.12460

SPECIAL ISSUE: NATURE'S MICROBIOME

Characterizing the plasticity of nitrogen metabolism by the host and symbionts of the hydrothermal vent chemoautotrophic symbioses *Ridgeia piscesae*

LI LIAO,*† SCOTT D. WANKEL,‡ MIN WU,§ COLLEEN M. CAVANAUGH* and PETER R. GIRGUIS*

*Department of Organismic and Evolutionary Biology, Harvard University, 16 Divinity Ave, Cambridge MA, 02138-2020,USA, †SOA Key Laboratory for Polar Science, Polar Research Institute of China, Shanghai 200136, China, ‡Department of Marine Chemistry and Geochemistry, Woods Hole Oceanographic Institution, 266 Woods Hole Rd., MS 25, Woods Hole, MA 02540, USA, §College of Life Sciences, Zhejiang University, 388 Yuhangtang Road, Hangzhou 310058, China

Abstract

Chemoautotrophic symbionts of deep sea hydrothermal vent tubeworms are known to provide their hosts with all their primary nutrition. While studies have examined how chemoautotrophic symbionts provide the association with nitrogen, fewer have examined if symbiont nitrogen metabolism varies as a function of environmental conditions. *Ridgeia piscesae* tubeworms flourish at Northeastern Pacific vents, occupy a range of microhabitats, and exhibit a high degree of morphological plasticity [e.g. long-skinny (LS) and short-fat (SF) phenotypes] that may relate to environmental conditions. This plasticity affords an opportunity to examine whether symbiont nitrogen metabolism varies among host phenotypes. LS and SF *R. piscesae* were recovered from the Axial and Main Endeavour Field hydrothermal vents. Nitrate and ammonium were quantified in *Ridgeia* blood, and the expression of key nitrogen metabolism genes, as well as stable nitrogen isotope ratios, was quantified in host branchial plume and symbiont-containing tissues. Nitrate and ammonium were abundant in the blood of both phenotypes though environmental ammonium concentrations were, paradoxically, lowest among individuals with the highest blood ammonium. Assimilatory nitrate reductase transcripts were always below detection, though in both LS and SF *R. piscesae* symbionts, we observed elevated expression of dissimilatory nitrate reductase genes, as well as symbiont and host ammonium assimilation genes. Site-specific differences in expression, along with tissue stable isotope analyses, suggest that LS and SF *Ridgeia* symbionts are engaged in both dissimilatory nitrate reduction and ammonia assimilation to varying degrees. As such, it appears that environmental conditions –not host phenotype—primarily dictates symbiont nitrogen metabolism.

Keywords: hydrothermal vent, nitrogen, *Ridgeia*, symbiosis, tubeworm

Received 1 May 2013; revision received 26 June 2013; accepted 27 June 2013

Introduction

Deep sea hydrothermal vents are often dominated by large animals that are obligately symbiotic with chemoautotrophic bacteria (Stewart & Cavanaugh 2006). Many of the hosts in these associations are entirely dependent upon their symbionts (microbiome) for nutrition. Indeed, the reduction of the host gut prevents the uptake and ingestion of particulate organic matter, and hosts are incapable of completing their life cycles without their symbionts. The uptake of dissolved organic matter by such symbioses may still be possible (Fiala-Médioni *et al.* 1986) but is unlikely to substantially contribute to the nutritive needs of the association.

The vestimentiferan tubeworms (phylum Annelida, family Siboglinidae) are among the best-studied chemoautotrophic symbioses and are abundant at vents along

Correspondence: Peter R. Girguis;
E-mail: pgirguis@oeb.harvard.edu

the East Pacific Rise (EPR; Jones 1985; Black *et al.* 1997; Stewart & Cavanaugh 2006), the Juan de Fuca Ridge (JDF; Southward *et al.* 1995; Black *et al.* 1997; Stewart & Cavanaugh 2006) and other vent and cold seep sites. Adult tubeworms are mouthless and gutless, and host intracellular chemoautotrophic symbionts (γ-proteobacteria) live densely in a specialized organ called the trophosome (Cavanaugh *et al.* 1981). It is thought that tubeworms rely on their symbionts for all their primary nutrients, including carbon, nitrogen, and phosphorous (Stewart & Cavanaugh 2006; Gibson *et al.* 2010). Several tubeworm genera are found at hydrothermal vents, including *Riftia*, *Ridgeia*, *Oasisia* and *Tevnia* (as reviewed in, Gibson *et al.* 2010). All vent tubeworm symbionts are closely related, with nearly identical 16S rRNA gene sequences (Feldman *et al.* 1997; Di Meo *et al.* 2000; Harmer *et al.* 2008) and strikingly similar metagenomes (Gardebrecht *et al.* 2011).

Living at the interface between cold seawater and warm vent fluids, tubeworms use their plume-like gill to take up reduced chemicals (e.g. sulphide) from the vent fluid and oxygen from the ambient seawater, providing substrates for energy generation by the sulphide-oxidizing symbionts. In exchange, symbionts use the energy derived from sulphide oxidation to fix CO_2 into organic carbon to feed themselves and their hosts (Felbeck *et al.* 1981; Felbeck & Jarchow 1998).

While carbon and energy metabolism in tubeworm symbioses are well studied (Felbeck *et al.* 1981; Fisher & Childress 1986; Childress *et al.* 1991; Goffredi *et al.* 1997; Felbeck & Jarchow 1998; Girguis & Childress 2006; Nyholm *et al.* 2008; Scott *et al.* 2012), modes of nitrogen metabolism have been less studied (Hentschel & Felbeck 1993; Pospesel *et al.* 1998; De Cian *et al.* 2000; Girguis *et al.* 2000). The growth and maintenance of any organism requires an exogenous nitrogen source, and at hydrothermal vent, the dissolved organic nitrogen (i.e. amino acids) is scarce, usually <200 pM (Johnson *et al.* 1988; De Cian *et al.* 2000). As mentioned, the lack of a mouth and a gut prevents ingestion of particular organic matter. Inorganic nitrogen, however, is abundant in the surrounding seawater, including dissolved dinitrogen (approximately 590 μM) and nitrate (approximately 40 μM; Charlou *et al.* 2000; Bourbonnais *et al.* 2012). Also, ammonium is present at some vents, and its concentrations range widely from <1 μM at the East Pacific Rise (Minic & Hervé 2003) up to 640–950 μM along the Endeavour segment of the Juan de Fuca Ridge (Lilley *et al.* 1993) and approximately 15 mM at the sedimented vents in the Guaymas Basin (Von Damm *et al.* 1985; Karl *et al.* 1988). The elevated concentrations of ammonium probably result from the decomposition of organic substrates in sediments buried in the subseafloor or covering the ridge axis.

Around hydrocarbon and brine seeps, environmental ammonium is known to be an important nitrogen source for chemoautotrophic symbioses (Lee & Childress 1994; Lee *et al.* 1999). However, the extent to which vent chemoautotrophic symbioses use ammonium is unclear. Most previous studies suggest that *Riftia* symbionts are engaged in dissimilatory nitrate reduction (Hentschel & Felbeck 1993; Gardebrecht *et al.* 2011; Markert *et al.* 2011), assimilatory nitrate reduction (Lee & Childress 1994) or dissimilatory nitrate reduction to ammonium (DNRA) as a source of reduced nitrogen for biosynthesis (Girguis *et al.* 2000). Modest ammonium assimilation by *Riftia* worm tissues has also been observed (Lee & Childress 1994; Minic *et al.* 2001), and *Riftia* living in organic-rich sedimented hydrothermal vents use ammonium rather than nitrate (Robidart *et al.* 2011). Sedimented vent systems aside (which are anomalous due to the high concentrations of organic matter), it is unclear whether chemoautotrophic symbioses living at the more common basaltic vents are engaged in nitrate reduction even in the presence of exogenous ammonium. Moreover, it is unclear if there are variations in nitrogen uptake and utilization by the same species living in different microhabitats, for example, warmer or cooler diffuse vents where nitrate and ammonium concentrations can be drastically different.

Ridgeia piscesae vent tubeworms (hereafter referred to simply as *Ridgeia;* Fig. 1A, B) are an ideal model to investigate nitrogen utilization because they are found in a broad range of habitats at vents in the Northeast Pacific, thriving in environments with a wide range of exogenous ammonium concentrations (from approximately 10 to >950 μM; Black *et al.* 1998). *Ridgeia* also exhibit two distinct phenotypes, hereafter referred to as long-skinny (LS) and short-fat (SF) *Ridgeia*. LS and SF *Ridgeia* are strikingly different in size, tube shape and colour, and plume shape. The LS morphotype tend to be narrow and long, *c.* 20–30 cm in length, with an extensive root-like posterior (Southward *et al.* 1995; Andersen *et al.* 2006; Carney *et al.* 2007). They typically weigh 1–5 g (wet weight, without the tube). SF *Ridgeia* are typically shorter, *c.* 5–10 cm in length, with a larger aspect ratio and without a root-like posterior. They typically weigh 2–15 g (wet weight, without the tube). *Ridgeia* symbionts are identical at the 16S rRNA level among the different phenotypes and are closely related to *Riftia* symbionts (approximately 99% identity of 16S; Feldman *et al.* 1997; McMullin *et al.* 2003). LS and SF *Ridgeia* dominate different microhabitats, with LS *Ridgeia* commonly found on basalts around low temperature vent fluids and SF *Ridgeia* commonly found on chimneys with higher temperature fluids (Urcuyo *et al.* 1998; Andersen *et al.* 2006). Even when both phenotypes occur in the same aggregation, they occupy different microhabitats (SF *Ridgeia* are in the middle bathed in

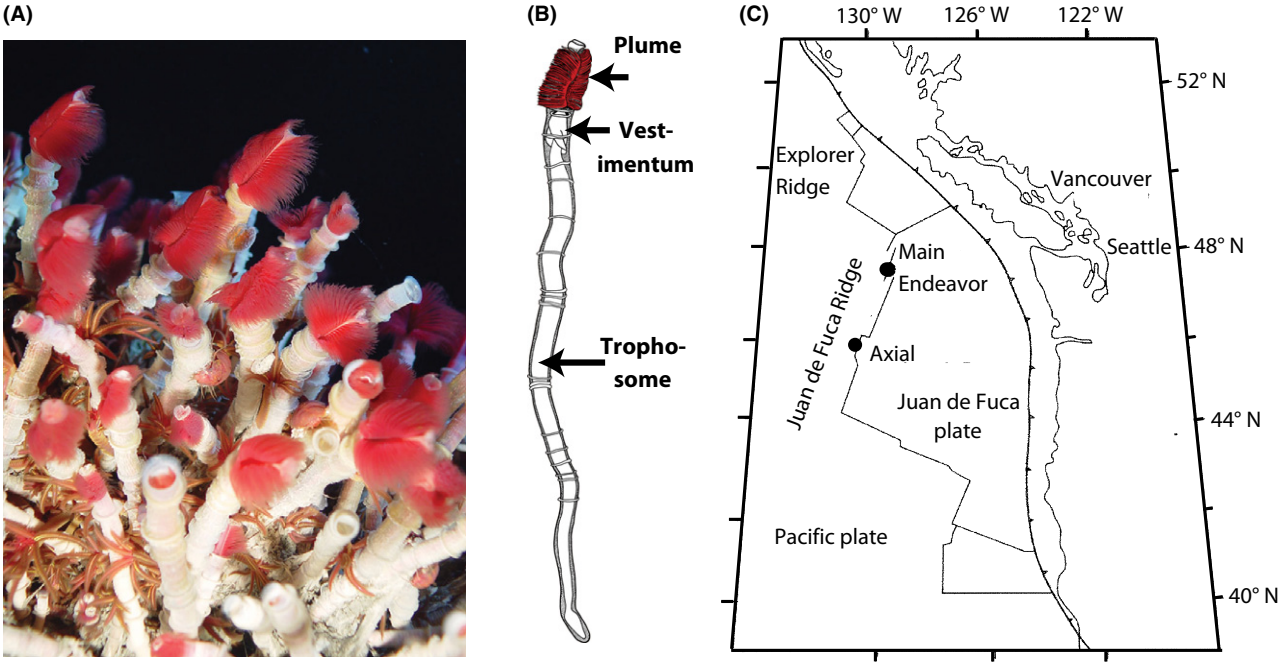

Fig. 1 (A) Photograph of *Ridgeia piscesae* tubeworms flourishing at a vent along the Juan de Fuca Ridge (courtesy of V. Tunnicliffe and CSSF); (B) A schematic of a generic *Ridgeia piscesae* tubeworm, illustrating gross morphology and the general locations of the plume, vestimentum, and trophosome, the organ housing the chemoautotrophic symbionts deep within the worm; (C) Map showing the locations of the Axial and Main Endeavour vent fields, from which *Ridgeia* were collected. Adapted from (Ding *et al*. 2001).

warmer fluids, whereas LS *Ridgeia* are on the periphery in cooler fluids; personal observation). It has been proposed that physical and chemical differences in their microhabitats may be responsible for the morphological difference in tubeworms (Black *et al*. 1994; Carney *et al*. 2007). For example, LS *Ridgeia*, with their root-like posteriors, may flourish in cooler regimes as they are able to access chemically reduced vent fluids in the subseafloor via the 'roots' (Urcuyo *et al*. 2003). Given the likely differences in the nitrogen regime in these cooler and warmer sites, we hypothesized that nitrogen utilization may differ between the two phenotypes and among vent sites, and that differences in the nitrogen source will be manifested as differences in nitrogen metabolism. Moreover, this would likely be reflected in differences in the stable nitrogen isotope ratios of the association (which, in turn, is relevant to understanding trophic structure among organisms living within or near *Ridgeia* aggregations).

Here, we present the results of a study on nitrogen metabolism by *Ridgeia* collected from the Main Endeavour Field (MEF) and the Axial hydrothermal vents during expeditions in 2010 and 2011 (Fig. 1C). We sampled both LS and SF *Ridgeia* phenotypes and determined both nitrate and ammonium concentrations in *Ridgeia* blood. Gene expression of key enzymes involved in symbiont dissimilatory nitrate reduction (*narG* and *napA*), symbiont assimilatory nitrate reduction (*nasA*), as well as symbiont and host ammonium assimilation (*glnA* and *gltB*) was investigated using quantitative reverse transcription PCR (qRT–PCR). The following experiments were aimed at addressing whether differences in nitrogen metabolism can be discerned from differences in host blood nitrate and ammonium concentrations, as well as gene expression, between these two phenotypes recovered from geochemically distinct sites. We specifically sought to determine whether potential differences in the availability of nitrogenous compounds within microhabitats influenced the utilization of nitrogen sources by the *Ridgeia* symbiosis, and whether there are consistent differences in the patterns of gene expression and stable nitrogen isotope ratios between the two phenotypes, which shed light on their respective forms of nitrogen acquisition.

Materials and methods

Sample collection and environmental condition

SF and LS *Ridgeia* tubeworms were collected from hydrothermal vent sites at the Main Endeavour Field (MEF) on the Juan de Fuca (JDF) and the Ashes vent field at the Axial volcano caldera (Fig. 1C). Both SF and LS *Ridgeia* were recovered from diffuse vents found near the Hulk massive sulphide deposit (located at the northern edge of the MEF) using the *DSV Alvin* during

dive 4619 in July 2010. Temperatures among the SF *Ridgeia* were approximately 17 °C, while temperatures among the LS *Ridgeia* were approximately 5 °C. Samples from the Ashes vent field were collected using the remotely operated vehicle *Doc Ricketts* during dives 257 and 258 in July 2011. At Ashes, LS *Ridgeia* and SF *Ridgeia* were found in the same aggregations, and LS *Ridgeia* were characteristically found along the periphery while SF *Ridgeia* were in the middle (i.e. closer to the venting fluid). Temperatures recorded at Ashes were approximately 24 °C among the SF *Ridgeia* and approximately 5 °C among the LS *Ridgeia*. To mimic vent-like conditions during return to the surface (thereby minimizing the changes in mRNA transcripts), all *Ridgeia* tubeworms collected were placed into a novel sampling device consisting of a 5-L container prefilled with red-dyed seawater containing 150 μM sulphide at pH 6.5. The water-tight (though not pressure-tight) container was kept sealed and insulated during descent, and the red food colouring allowed us to visually confirm that sulphidic water remained around the samples during ascent and recovery. Upon recovery, the sulphide concentration was approximately 40% less due to dilution while sampling. On board ship, samples were rapidly dissected into gill, vestimentum, and trophosome (without the body wall), and sections were flash-frozen in liquid nitrogen for RNA extraction.

Nitrate and ammonium concentrations in blood

Vascular and coelomic fluids were taken from select *Ridgeia* by using a fresh syringe and 28-ga. hypodermic needle. Freshly collected blood was flash-frozen in liquid nitrogen. Blood nitrate concentrations were determined based on the integrated peak area on a mass spectrometer by using the denitrifier method (Sigman *et al*. 2001). Standards of known amounts of nitrate were used to calibrate the mass spectrometer's response. Analyses were carried out in the laboratory of Prof. Dr. Moritz Lehmann at the University of Basel, Switzerland. Blood ammonium concentrations were determined by diluting blood samples to 1:10 or 1:100 in DI water, and then using standard flow injection analyses with the indophenol method (Lee & Childress 1994) at the Marine Science Institute Analytical Lab at University of California, Santa Barbara.

RNA extraction and reverse transcription

Four LS and six SF *Ridgeia* from the MEF site, and four of each phenotype from the Axial site, were used for RNA extraction. Approximately 25 mg of flash-frozen trophosome and plume tissues from each individual were dissected on dry ice and equilibrated in 500 μL of RNAlater®-ICE (Ambion) at 4 °C overnight. Total RNA was extracted from each tissue using RNeasy mini kit (QIAGEN), following the manufacturer's protocol. Afterwards, RNA was eluted in 50 μL of RNase-free water. RNA was treated with DNase using the Turbo DNA-free kit (Ambion) and further checked for DNA contamination by PCR using primers for *R. piscesae* host glutamine synthetase (GS), as described below. RNA integrity was assessed on a 2100 Bioanalyzer (Agilent). The purity and quantity of RNA was checked using a fluorometric assay for RNA concentrations (Qubit RNA BR assay on a Qubit 2.0 fluorometer; Life Technologies). Upon completion, up to 1 μg of total RNA was reverse-transcribed to cDNA by using qScript cDNA SuperMix (Quanta Biosciences), containing random primers and oligo(dT) primers. cDNA was stored at −80 °C for further use.

Primer design and validation

Quantitative RT–PCR primers were designed for select functional genes that represent key nitrogen metabolisms, as well as for candidate reference genes (Table 1, Fig. 2). Specifically, to interrogate nitrate utilization by the symbiont, we designed primers for genes encoding dissimilatory nitrate reductases (*narG* and *napA*) and assimilatory nitrate reductase (*nasA*). To investigate ammonium assimilation by symbionts and hosts, we designed specific primers for symbiont and host glutamine synthetase and glutamate synthase (*glnA* and *gltB*, respectively). Four housekeeping genes (HKG) including *rpoA*, *cysG*, *gyrB*, and *mraY* were carefully chosen from different functional groups to avoid coregulation (Table 1). Because symbionts of tubeworm genera exhibit high DNA sequence identity, all symbiont primers were designed against the published metagenomes of *Riftia pachyptila* and *Tevnia jerichonana* symbionts (Markert *et al*. 2007; Gardebrecht *et al*. 2011) using the software program Primer Premier 5 (Premier Biosoft International), and then checked via the BLASTn for specificity. *Ridgeia* host primers were based on ESTs recovered in a previous study (available via www.ncbi.nlm.nih.gov/; Nyholm *et al*. 2008). To validate their efficiency in *Ridgeia*, endpoint PCR was performed using all primers and cDNA as template, and the resulting amplicons were confirmed by Sanger sequencing.

Quantitative RT–PCR

Quantitative RT–PCR (qRT–PCR) was performed using a Stratagene Mx3005P realtime thermal cycler (Agilent Technologies). Plasmid standards were made by cloning target amplicons into pSC-B vectors (Strataclone Blunt PCR Cloning Kit, Agilent Technologies) and then sequenced to validate the inserts. Recombinant plasmids were linearized by restriction enzyme *Hind*III digestion

Table 1 Primers designed for functional and reference genes used for quantitative RT–PCR

Gene	Product	Forward primer (5′–3′)	Reverse primer (5′–3′)	Amplicon size (bp)
Ridgeia piscesae host gene				
Ammonium assimilation				
$glnA_{\mathrm{Rid}}$	Glutamine synthetase (GSII), large subunit	CGGTCGTGAGGTGATGG	TTCGTGCTGAAGTTCGTGT	264
$gltB_{\mathrm{Rid}}$	Glutamine synthetase (GOGAT), large subunit	TGTCGCAGTTTATGTTTCC	TACCAGCACAAGCAGTCC	137
Reference				
*ACTB**	β-actin	ACAGAAGGACAGCTATGTCG	TGTCATCCCAGTTTGTGACG	105
Ridgeia piscesae symbiont gene				
Ammonium assimilation				
$glnA_{\mathrm{sym}}$	Glutamine synthetase (GSI), large subunit	AGATGTTTGGATGGCTCCTCC	CTCGAGGATGTCGCAGCGTA	141
$gltB_{\mathrm{sym}}$	Glutamine synthetase (GOGAT), large subunit	GCACGGGTACGCCACTCCAC	GTCGGCGTGGGCCTTGGAAA	198
Nitrate assimilation				
nasA	Cytoplasmic nitrate reductase, catalytic subunit	TGCCTTCGCCATCATCTCTA	CGCTCCTGTGCCTCTTTCAT	276
Nitrate respiration				
napA	Periplasmic nitrate reductase, catalytic subunit	GAAGATGTATGGCCGGAGGAT	GAACAGACCCTTCTGTGCGTAA	192
narG	Membrane-bound nitrate reductase, catalytic subunit	TGGGTCGAGGCGGGGTCAAT	AGGATGCCGCCACGCTTACC	155
Reference				
rpoA	DNA-directed RNA polymerase alpha subunit	TCGACAGAGTTCGGCGGGTGAA	GCTGCTCAACACGCGCAGATT	113
cysG	Uroporphyrinogen-III C-methyltransferase	ATCGCCGAGTTGGCTGAGG	AGGCTTGTGGAAGGTCGTTTT	252
gyrB	DNA gyrase subunit B	ACTGCGCTTGAGAATTCGGCG	TCGGCCAACCAGCCATCCAT	221
mraY	Phospho-N-acetylmuramoyl-pentapeptide-transferase	GGCTTGATCGCCCGTTGGAA	ATCACAGTGGGCAGGATCGCCA	242

*Primers for *ACTB* were designed by Nyholm *et al.* (2012). All other primers were designed in this study.

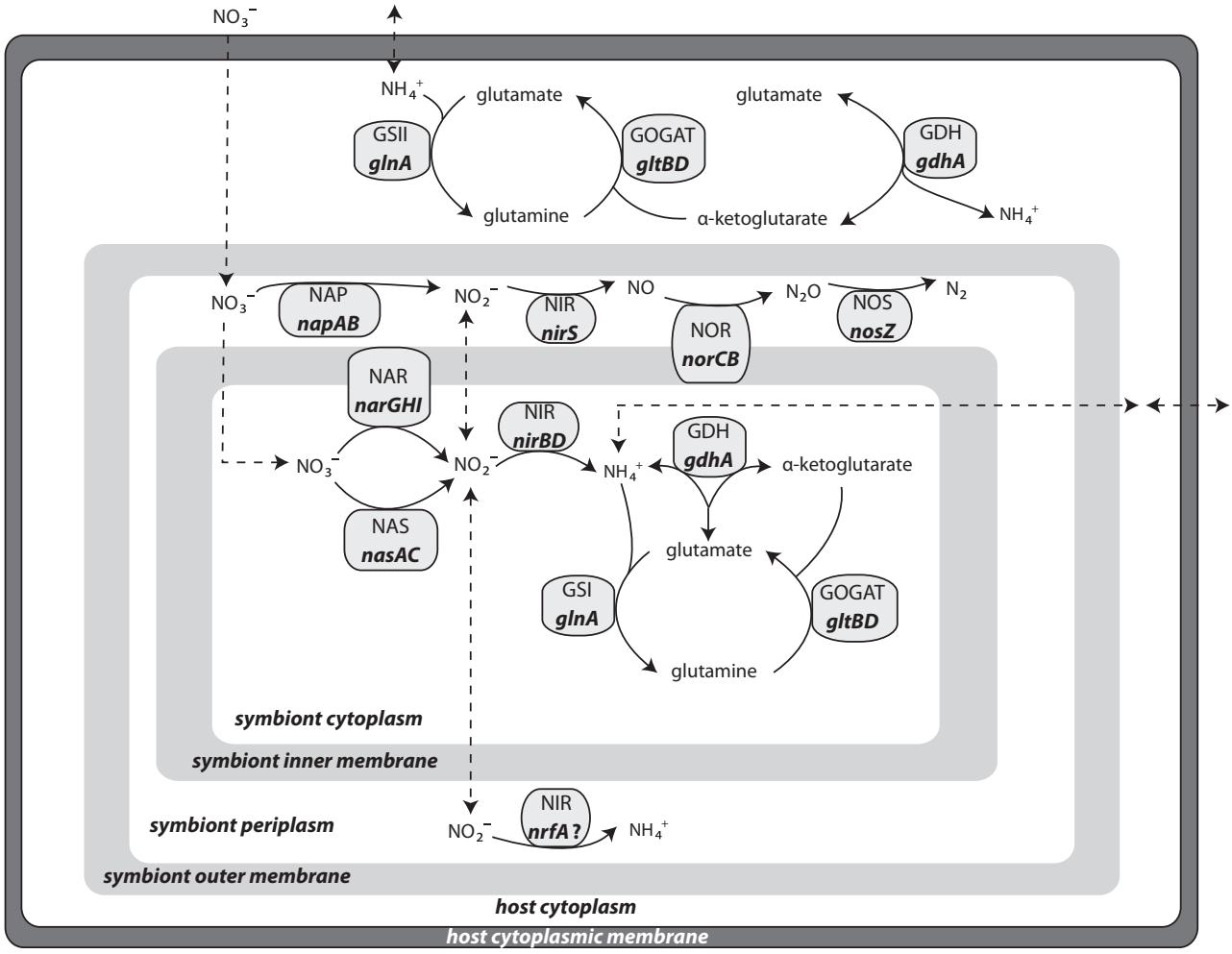

Fig. 2 Schematic representing potential modes of nitrogen acquisition and utilization based on genes encoded in the symbiont genomes of *Riftia pachyptila* and *Tevnia jerichonana* (Markert *et al.* 2011, Gardebrecht *et al.* 2012). Enzymes (capitals) and corresponding structural genes (bold italics; first capital letter as the large subunit) are listed in grey boxes. Dashed lines indicate metabolite diffusion or transport. Question marks denote genes missing in the metagenomes. NAP: periplasmic nitrate reductase, NIR: periplasmic nitrite reductase, NOR: nitric oxide reductase, NOS: nitrous oxide reductase, NAR: periplasmic nitrate reductase, NAS: assimilatory nitrate reductase, NIR: cytoplasmic nitrite reductase and NRF: direct reduction from nitrate to ammonium. For ammonium assimilation genes, see Table 1.

and subsequently quantified using a fluorometric assay (the Qubit DNA BR assay; Life Technologies). Standards were constructed by serial dilution of linearized plasmids. The qRT–PCR reaction mixture (20 μL) contained a final concentration of 1× PerfeCTa SYBR Green FastMix (Quanta Biosciences), 300 nM of each primer, and 2 μL of template (32–122 ng). Three-step qPCR cycles were used: 95 °C for 10 min; 40 cycles of 95 °C for 30 s, 60 °C for 30 s, 72 °C for 30 s; followed by melting curve analyses to confirm the absence of nonspecific amplification. Fluorescence data collected during the annealing stage of amplification were analysed by the manufacturer's software. Efficiency was calculated based on the standard curves. Inhibition in samples for qRT–PCR was tested by comparing C_t values of plasmid standard-only reaction to plasmid spiked with cDNA sample. No template controls (NTC) and non-RT controls were run under same conditions to ensure the absence of contamination and genomic DNA, respectively.

Reference gene validation and data analyses

To compare samples, host and symbiont functional gene expressions were normalized to a reference gene. For the host, the β-actin gene *ACTB* was used as a reference (as in Nyholm *et al.* 2012). For the symbionts, four bacterial reference genes were considered, and two different algorithms were used to evaluate their expression stability, geNorm (Vandesompele *et al.* 2002) and NormFinder (Andersen *et al.* 2004). Raw C_t values were log-transformed to copy numbers using standard curves of the four HKG as input data for geNorm calculation. The gene expression

stability value (M) for each gene was then calculated. Log-transformed copy numbers were calculated, and the housekeeping genes were then ranked according to the intra- and intergroup expression variation.

Raw C_t values of bacterial functional genes and HKG were transformed to copy numbers based on standard curves. Average copy numbers of triplicates from functional genes were normalized to those of the validated reference gene(s) for the hosts and the symbionts, respectively. The normalized data were used to calculate the fold change between *R. piscesae* phenotypes and vents. The nonparametric Mann–Whitney *U*-test was used to calculate significance between samples.

Nitrogen isotopic analyses

Trophosome tissues of SF *Ridgeia* from Axial and MEF and LS *Ridgeia* from MEF were freeze-dried, acidified, and then homogenized by bead-beating prior to $\delta^{15}N$ determination. Approximately 0.5 mg of homogenized tissue was analysed by combustion in an elemental analyzer coupled to an isotope ratio mass spectrometer. Values were normalized using internationally calibrated standards, N_2, with a precision of approximately 0.1‰.

Results

Nitrate and ammonium concentrations in blood

Nitrate was determined to be 109.8 ± 7.8 μM in LS *Ridgeia* blood (n = 5) and 91.8 ± 6.2 μM in SF *Ridgeia* blood (mean ± SE; n = 4). Nitrate concentrations were not significantly different between the two phenotypes (P > 0.05, Mann–Whitney *U*-test). Ammonium detected in the *Ridgeia* blood ranged from approximately 119 ± 4 (mean ± SE; n = 3) for the SF *Ridgeia* to >200 μM for the LS *Ridgeia* (n = 3). We are unable to provide a mean and SE for the LS *Ridgeia* blood samples because they were beyond the upper range of the analyzer (200 μM), and samples were expended prior to better quantification by dilution.

Endpoint PCR

Endpoint PCR products of nitrogen genes and references were sequenced using both forward and reverse primers and Sanger sequencing. The direct sequencing results matched sequences from *R. pachyptila* and *T. jerichonana* symbiont metagenomes (Gardebrecht *et al*. 2011). Symbiont primers did not show cross-reactivity with host plume RNA. Via endpoint PCR, we did not detect genomic DNA contamination in the total RNA treated with DNase. Moreover, all non-RT controls did not amplify. cDNA, however, amplified with host $glnA_{\mathrm{Rid}}$ primers showed a single band of 264 bp on an agarose gel. Because $glnA_{\mathrm{Rid}}$ primers cross intron(s), yielding a PCR amplicon near 1000 bp using genomic DNA as template, these results confirmed that no genomic DNA was present in the RNA samples.

Standard curve and efficiency for qRT–PCR

Plasmids containing target gene inserts were used as standards. Ten-fold serial dilutions of standards were included to cover a range of C_t from approximately 10–30. Efficiencies of the assays ranged from 90% to 111% (Table 2). Specific amplification was confirmed by melting curve analyses, which revealed a single melting peak for each primer set, indicating a single PCR prod-

Table 2 Percent efficiency and other details for the quantitative qPCR assays. Data shown are derived from analyses of the standard curves

Gene	Efficiency (%)	Y-intercept	R^2	C_t of NTC*	Slope	Threshold
narG	106.2	35.00	1.000	No C_t	−3.182	0.8205
napA	101.7	33.84	0.999	No C_t	−3.283	0.6752
nasA	102.1	34.06	1.000	No C_t	−3.272	0.9635
$glnA_{\mathrm{sym}}$	107.0	33.89	1.000	No C_t	−3.165	0.7804
$gltB_{\mathrm{sym}}$	104.0	33.53	0.999	No C_t	−3.229	0.6907
rpoA	109.0	35.25	0.999	38.75	−3.123	0.7765
cysG	105.5	33.37	1.000	No C_t	−3.197	0.9201
gyrB	107.6	33.18	1.000	No C_t	−3.153	0.7976
mraY	101.2	34.13	1.000	No C_t	−3.293	0.7947
$glnA_{\mathrm{Rid}}$	91.6	37.15	0.998	No C_t	−3.541	0.8929
$gltB_{\mathrm{Rid}}$	103.7	34.35	1.000	39.99	−3.237	0.8183
ACTB	103.2	35.23	0.997	No C_t	−3.248	0.7355

*No template control.

uct. Electrophoresis analysis of all amplicons from qPCR also showed a single band with the expected sizes. No primer dimers were observed.

Reference genes and normalization

Both *mraY* and *rpoA* were found to be the best reference genes by geNorm, while *mraY* was the best reference as determined by NormFinder (NF; Fig. 3). Notably, the same patterns of relative gene expression were observed via both genes, supporting the use of either normalization method. All functional genes from symbionts at the Axial site were normalized to *mraY* using NF. Due to limitations in template, functional genes from symbionts at the MEF were normalized to *mraY*. Host genes from all samples were normalized to the β-actin gene (*ACTB*) as previously described (Nyholm *et al.* 2012).

Nitrate reductase gene expression in the symbionts

The periplasmic nitrate reduction gene, *napA*, was expressed at similar levels in the LS and SF symbionts from both the Axial and MEF (Fig. 4). On average, *napA* expression was approximately 3-fold higher than the reference gene, *mraY*, in both phenotypes at both sites (Fig. 4). The nitrate respiration gene, *narG*, was detected in symbionts from both LS and SF *Ridgeia* at the MEF (approximately 2-fold higher than *mraY* gene on average). However, *narG* was below the limits of detection in *Ridgeia* symbionts from the Axial site (Fig. 4A). The expression of assimilatory nitrate reductase (*nasA* gene) was not detected in any individuals from any sites.

Ammonium assimilation gene expression in the symbionts

Genes involved in ammonium assimilation were highly expressed in the LS and SF symbionts at both vent sites (Fig. 4). However, LS *Ridgeia* symbionts had the highest expression of glutamine synthetase gene, $glnA_{sym}$, 68- and 31-fold higher than periplasmic nitrate reductase gene, *napA*, at the Axial and MEF, respectively. In contrast, SF *Ridgeia* symbionts showed 4- and 11-fold higher expression of $glnA_{sym}$ than *napA* on average at the Axial

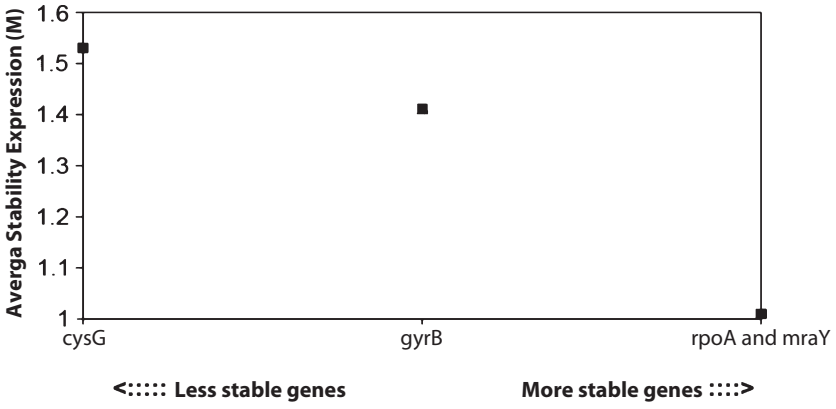

Fig. 3 Bacterial reference genes as ranked by the software program geNorm. Two genes, *mraY* and *rpoA*, were recommended for normalization.

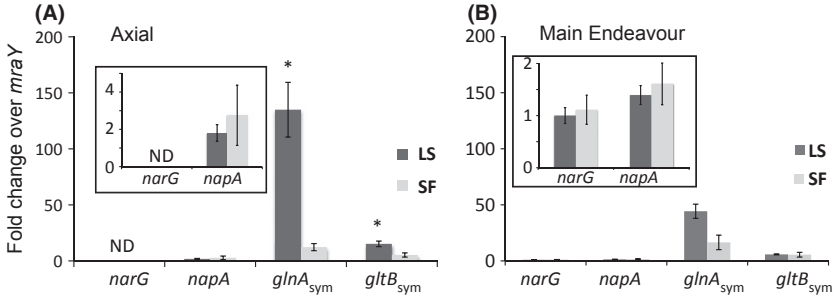

Fig. 4 Relative abundance of functional genes expressed in Ridgeia symbionts (mRNA) and normalized to reference gene *mraY* from the Axial (A) and Main Endeavour (B) vent sites. Insets show relative abundance of narG and napA on a smaller scale for better visualization. The *y*-axes denote the relative ratio with respect to the reference gene, *mraY*. Asterisks indicate statistical significance between LS and SF *Ridgeia* ($P < 0.05$, Mann–Whitney *U*-test). LS: long-skinny *Ridgeia*; SF: short-fat *Ridgeia*. A description of gene names may be found in Table 1. The subscript 'sym' denotes symbiont genes. ND = not detected.

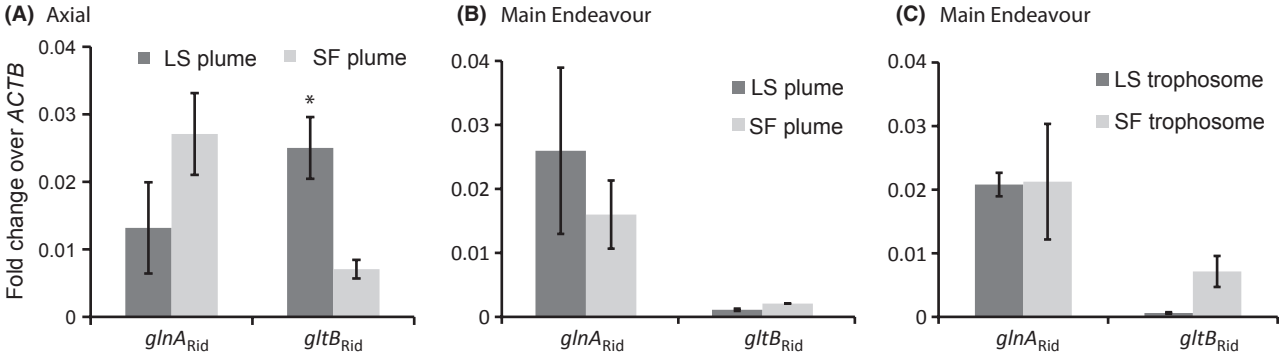

Fig. 5 Relative abundance of host functional genes (mRNA) normalized to reference gene *ACTB* in *Ridgeia* recovered from the Axial and Main Endeavour vent field (MEF). (A) Data shown are from the plume tissue of *Ridgeia* collected at the Axial site. (B) data from the plume tissue of *Ridgeia* collected at the MEF. (C) data from the trophosome tissue of *Ridgeia* collected at the MEF. Asterisk indicates statistical significance between LS and SF *Ridgeia* ($P < 0.05$, Mann–Whitney *U*-test). A description of gene names may be found in Table 1. The subscript 'Rid' denotes host genes.

and MEF, respectively. $glnA_{sym}$ expression was significantly different between LS and SF symbionts at the Axial site, with LS being higher ($P < 0.05$; Fig. 4A). Expression of glutamate synthase, or $gltB_{sym}$, in LS symbionts was 15- and 6-fold higher than *napA* at the Axial site and the MEF, respectively. However, expression of $gltB_{sym}$ in SF *Ridgeia* symbionts was only 3- and 2-fold higher than *napA* at the Axial site and the MEF, respectively. Expression of $gltB_{sym}$ was significantly different between LS and SF *Ridgeia* symbionts at the Axial site ($P < 0.05$; Fig. 4A). However, SF *Ridgeia* symbiont genes showed no significant differences across the two sites.

Ammonium assimilation gene expression in hosts

Ridgeia glutamine synthetase ($glnA_{Rid}$) and glutamate synthase ($gltB_{Rid}$) genes were expressed in all individuals at both sites (Fig. 5). Host $glnA_{Rid}$ showed comparable expression in both LS and SF *Ridgeia* plume/trophosome tissues across vent sites. However, $gltB_{Rid}$ showed a significant difference in expression between LS and SF hosts at the Axial site ($P < 0.05$; Fig. 5). No significant difference was found for $glnA_{Rid}$ and $gltB_{Rid}$ in plume and trophosome tissues at the MEF.

Nitrogen isotopic analysis of tissue

$\delta^{15}N$ was measured on trophosome tissue samples from SF ($n = 13$) and LS ($n = 10$) *Ridgeia* at MEF, as well as from SF *Ridgeia* at Axial ($n = 6$). SF *Ridgeia* at Axial had the lowest $\delta^{15}N$, $-2.7‰ \pm 0.6$, while $\delta^{15}N$ of SF *Ridgeia* at MEF were markedly higher, $+1.6‰ \pm 0.3$ (Fig. 6). LS *Ridgeia* at MEF had the highest $\delta^{15}N$ ($+3.7‰ \pm 0.5$). $\delta^{15}N$ was depleted in SF *Ridgeia* trophosome tissues from both sites, relative to the nitrogen isotopic composition of the NH_4^+ (+6.7‰ and +3.6‰ at Axial and MEF vent fluids, respectively) and NO_3^- (+5.6‰ in seawater across sites; Fig. 6; Bourbonnais *et al.* 2012). However, LS *Ridgeia* exhibited the same $\delta^{15}N$ as NH_4^+ in the vent fluids at MEF.

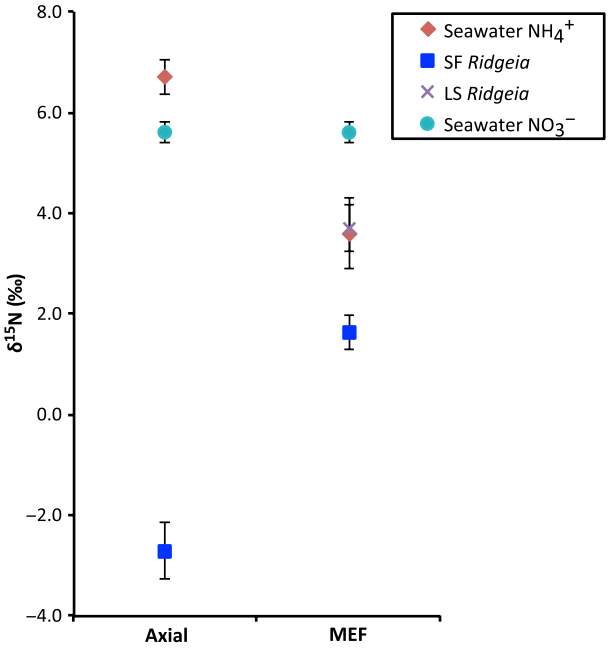

Fig. 6 Stable nitrogen isotope ratios ($\delta^{15}N$) of SF *Ridgeia* trophosome tissues from Axial ($n = 6$) and Main Endeavour Field (MEF; $n = 13$), as well as *Ridgeia* LS trophosome tissues from MEF ($n = 10$). Due to technical challenges, we were unable to recover the data from LS *Ridgeia* collected at Axial, and as such they are not presented here. $\delta^{15}N$ values for diffuse vent ammonium and nitrate measured previously at these sites are also shown(Bourbonnais *et al.* 2012). Seawater NH_4^+ = $\delta^{15}N$ of diffuse vent ammonium, SF *Ridgeia* = $\delta^{15}N$ of SF *Ridgeia* trophosome, LS *Ridgeia* = $\delta^{15}N$ of long-skinny *Ridgeia* trophosome and Seawater NO_3^- = $\delta^{15}N$ of diffuse vent nitrate.

Discussion

In general, the most readily available form of (inorganic) nitrogen in the deep sea –including around vents — is nitrate, which is found at approximately 40 μM worldwide. Many bacteria rely on nitrate for biosynthesis of nitrogen-containing compounds, typically via assimilatory nitrate reductase (Richardson *et al.* 2001; Kraft *et al.* 2011). Curiously, our data suggest that nitrate was not assimilated by *Ridgeia* symbionts via assimilatory nitrate reductases. Moreover, Nas has not been detected in previous studies of transcripts or peptides, even though *nasA* was found in the genome (Markert *et al.* 2007; Robidart *et al.* 2008; Gardebrecht *et al.* 2011). It has been previously shown that ammonium can repress *nasA* expression (Moreno-Vivián *et al.* 1999); thus, symbiont *nasA* may be absent due to the abundance of ammonium in the host blood from exogenous sources. Nevertheless, both the blood nitrate concentration (>90 μM) and symbiont gene expression data suggest that nitrate was being acquired and reduced. Indeed, the presence of nitrate in the blood at concentrations above those of the surrounding seawater also suggests that nitrate is being actively acquired by the host for use by the symbionts (the host, to our knowledge, cannot use nitrate for growth or biosynthesis). It has been suggested that *Riftia* possesses a nitrate-binding component in its blood (Hahlbeck *et al.* 2005), and this may also be true in *Ridgeia*.

Regardless, the periplasmic nitrate reductase *napA* was consistently expressed in symbionts across sites and phenotypes, and *narG* was also detected in the MEF *Ridgeia*, implicating the symbionts in nitrate metabolism. These data suggest that both phenotypes are engaged in denitrification. During denitrification, nitrate is typically reduced by these reductases to nitrite and ultimately to N_2. Although both Nar and Nap are involved in denitrification, they probably have different roles. Nar conserves energy *via* the generation of a proton motive force across the cytoplasm membrane (Richardson *et al.* 2001). In *Ridgeia* symbionts, *NarG* is possibly involved in catalysing the oxidation of sulphide using nitrate as a terminal electron acceptor. Nitrate respiration might 'supplement' oxygen under hypoxic or anoxic conditions (Girguis *et al.* 2000) and may reduce competition with the host for O_2 (though this remains to be thoroughly tested). Nap is canonically involved in redox balancing by disposing of excess reductant for the reoxidation of NADH, especially during fast growth under sufficient energy and oxygen conditions (Richardson *et al.* 2001). In *Ridgeia* symbionts, *napA* may be involved in redox balancing when metabolic rates are high (*Ridgeia* are known to exhibit high metabolic and growth rates, comparable to *Riftia*; Urcuyo *et al.* 1998, 2007; Nyholm *et al.* 2012), or when changes in the geochemical regime lead to physiological redox imbalances (Johnson *et al.* 1988; Wankel *et al.* 2011). Alternatively, nitrate reduction by Nap or Nar may be involved in the production of ammonium, analogous to dissimilatory nitrate reduction to ammonium, or DNRA (Simon 2002; Kraft *et al.* 2011). Although the gene encoding for Nir? (*nrfA*, Fig. 2), a cytochrome *c* nitrite reductase considered to be diagnostic for canonical DNRA (Simon 2002; Kraft *et al.* 2011), has not been identified in the *Riftia* and *Tevnia* symbiont genomes, our data reveal patterns of gene expression that offer another plausible mechanism by which ammonium resulting from the dissimilatory reduction of nitrate might be assimilated by the symbionts. As mentioned, both dissimilatory nitrate reductases *napA* and *narG*, as well as symbiont ammonium assimilation genes $glnA_{sym}$ and $gltB_{sym}$, were expressed (Fig. 4). *Ridgeia* may perform DNRA without *nrfA*, for example, possibly via periplasmic nitrate reductases, a transmembrane nitrite/nitrate transporter such as *narK*, cytoplasmic nitrite reductases and ammonium assimilatory pathways. Evidence for the expression of this assemblage of genes has been found in tubeworm symbiont metagenomes, transcripts, and peptides (Markert *et al.* 2007; Robidart *et al.* 2008; Gardebrecht *et al.* 2011), including *Ridgeia* (Nyholm *et al.* 2008) and other vent chemoautotrophic symbioses (Sanders *et al.* 2013). Indeed, mass balance and isotopic studies have implicated *Riftia* symbionts in DNRA (Girguis *et al.* 2000), although this previous study did not examine gene or protein expression to establish the physiological mechanisms underlying the observed DNRA. This represents a potential mechanism for assimilation of periplasmically reduced nitrate via the shuttling of nitrite into the cytoplasm for reduction to ammonium. Due to a lack of sufficient mRNA, we were unable to complete our assays for nitrite reductases, though they were detected in the cDNA via endpoint PCR (data not shown). As such, further studies are required to confirm whether ammonium observed in these *Ridgeia* was indeed produced via DNRA. We suggest that the confluence of these patterns in nitrogen gene expression among these taxa may suggest a convergence of traits that enable vent animal–microbial symbioses to use nitrate as both an oxidant and nitrogen source for biosynthesis, and future studies should further elucidate the details of this hypothesis.

Even though the aforementioned patterns of gene expression represent a plausible means by which an association can acquire nitrogen, acquisition of exogenous ammonium is another potential source of nitrogen at vents. Ammonium is present at both Axial (approximately 14 μM) and the MEF (>400 μM) sites, which are concentrations higher than many other basaltic vents

(Minic & Hervé 2003), as well as the ambient seawater (Bourbonnais *et al.* 2012). These are, however, the concentrations in pure vent fluid, and they will be markedly lower in the dilute fluids that surround the animal communities. Nevertheless, *Ridgeia* may be able to assimilate exogenous ammonium, which in turn may lead to lower rates of nitrate reduction. This is consistent with the very high levels of expression in symbiont $glnA_{sym}$, which are substantially higher than *napA* (up to 68-fold in the LS *Ridgeia* and 11-fold in the SF *Ridgeia*), although caution is always warranted when using gene expression levels as a representation of activity (and, as such, *glnA* expression does equal exogenous ammonia assimilation). While ammonium transporters are likely a better proxy for assimilation from the environment, their expression is known to be influenced by changes in environmental pH (which influences ammonia/ammonium speciation; Nakhoul *et al.* 2010). Given the dynamics of pH found at hydrothermal vents, we posited that expression of these transporters is heavily influenced by the dynamic changes for environmental pH. As such, we quantified both glutamine synthetase and glutamate synthase, for which expression was strikingly different among *Riftia* tubeworms living in ammonia-rich and poor environments (Robidart *et al.* 2011, Table S2).

Although SF and LS *Ridgeia* blood ammonium concentrations are comparable to those measured in *Riftia* (recovered from a low ammonium environment; De Cian *et al.* 2000), there are striking differences in the nitrate concentrations of *Ridgeia* and *Riftia* blood. As mentioned, *Ridgeia* concentrations were approximately 100 μM, whereas *Riftia* blood nitrate concentrations are typically between 300 nM and 3 mM (Hahlbeck *et al.* 2005). Also, in a previous study, *Riftia* from the Guaymas Basin (a sedimented vent field) took up ammonium in laboratory-based high-pressure studies and had much lower levels (9–24 times) of respiratory and assimilatory nitrate reductases than *Riftia* from the basaltic vents along the East Pacific Rise (Robidart *et al.* 2011).

In the light of these observations, we suggest that *Ridgeia* symbionts and host are engaged in some degree of ammonium assimilation from the environment. Of course, gene expression data do not reveal whether this ammonium is derived from symbiont nitrate reduction, from urea degradation (as in De Cian *et al.* 2000), or from exogenous organic sources, nor can one assume that these are mutually exclusive. Nevertheless, the substantially higher expression of ammonia assimilation genes in LS *Ridgeia*, which are not exposed to higher ammonia concentrations from vigorous venting around their branchial gills, suggests that they may be better poised to assimilate the ammonia from the deeper, interstitial fluids, using their 'roots' to access these fluids. This supposition is consistent with the observations presented here, but given the limitations of these data, it cannot be well substantiated.

Many studies have employed stable isotopic composition of N-bearing compounds and tissues to shed light on N sources and cycling mechanisms. In this study, the $\delta^{15}N$ of SF *Ridgeia* at Axial were lower than those found at MEF ($-2.7‰ \pm 0.6$ vs. $+1.6‰ \pm 0.3$; Fig. 6), with $\delta^{15}N_{NH4} - \delta^{15}N_{SF}$ values of 9.4‰ and 2.0‰ at Axial and MEF, respectively (Fig. 6). LS *Ridgeia* at MEF showed the same $\delta^{15}N$ ratios as the exogenous ammonium ($+3.7‰ \pm 0.5$). It is known that isotopic discrimination against ^{15}N during assimilation of ammonium or nitrate by microbes results in fractionation and the formation of biomass having a $^{15}N/^{14}N$ (or $\delta^{15}N$) lower than that of the substrate (Wada & Hattori 1978; Wada 1980; Cifuentes *et al.* 1989; Montoya *et al.* 1991; Montoya & McCarthy 1995). For nitrate assimilation, the fractionation (or $^{15}\varepsilon$, which is equal to $\delta^{15}N_{substrate} - \delta^{15}N_{product}$) stemming from nitrate reduction (e.g. NAR) is generally 5‰ when nitrate is not limiting (Waser *et al.* 1998; Needoba & Harrison 2004; Granger *et al.* 2010). Isotopic fractionation by ammonium assimilation is complicated by a number of chemical and biological processes, for example, isotopic equilibrium between ammonium and ammonia, as well as kinetic isotope effects by either of two intracellular ammonium assimilation pathways (Hoch *et al.* 1992; Waser *et al.* 1998). Nevertheless, the apparent $^{15}\varepsilon$ of ammonium assimilation does relate to environmental ammonium availability, with $^{15}\varepsilon$ values of approximately 27‰ when ammonium is high (e.g. tens of mM) and $^{15}\varepsilon$ values of approximately 4‰ when ambient ammonium is low (<1 mM). Collectively, these isotope data are consistent with less ammonium assimilation by SF *Ridgeia*. This is also consistent with the patterns of gene expression presented here. In aggregate with the gene expression data, these data suggest that LS *Ridgeia* are acquiring more ammonium directly from the environment, while SF *Ridgeia* may acquire N for biosynthesis via a unique dissimilatory nitrate reduction to ammonium, though as mentioned, this hypothesis remains to be substantiated. Of course, in these dynamic environments, N is assimilated by a combination of pathways – and the observed isotopic differences in the intact associations may simply be an integration of changes in physiological activity in response to changing environmental conditions.

We also observed differences in gene expression between the SF and LS phenotypes recovered from both sites. LS *Ridgeia* consistently had higher $glnA_{sym}$ expression than SF *Ridgeia*. Moreover, LS *Ridgeia* symbionts at the Axial site also exhibited higher $glnA_{sym}$ expression than the in LS *Ridgeia* symbionts from the MEF. If one

assumes that the warmer, more chemically reduced fluids around SF *Ridgeia* are more replete with ammonium, these data suggest that elevated expression of $glnA_{sym}$ in LS *Ridgeia* may reflect an increase in enzyme production to facilitate the acquisition of ammonium. Consistent with this suggestion is the aforementioned higher expression of $glnA_{sym}$ in LS *Ridgeia* symbionts.

Previous studies have shown that the expression of genes involved in nitrogen metabolism is, in part, governed by environmental nitrate and ammonium concentrations (Reitzer 2003). However, it is important to note that these studies examined free-living microbes in laboratory cultures. Prior to the data presented here, no study has attempted to characterize the relative influence of habitat variation vs. host phenotype on symbiont nitrogen metabolism. The resulting data herein reveal the complexities of nitrogen metabolism in the *Ridgeia* symbioses and underscore the physiological variations that may be seen in a host's microbiome, even among identical symbiont types living in association with two different host phenotypes. These data clearly suggest that all *Ridgeia* hosts take up nitrate, and their symbionts may use that nitrate via dissimilatory pathways as an electron acceptor for sulphide oxidation. However, there is circumstantial evidence to suggest that SF *Ridgeia* may also direct this nitrate to the production of ammonium for biosynthesis and growth via a process analogous to canonical DNRA. In contrast, the high representation of ammonium assimilation transcripts among LS *Ridgeia* suggests a sizable, if not major, role of exogenous ammonium as a nitrogen source for the symbiosis, especially in light of the relatively high concentration of ammonium at these vents. While additional investigations will be required to determine the fate of environmentally-derived nitrate and ammonium among both LS and SF *Ridgeia*, it is worth considering that the observed metabolic flexibility within the symbionts is analogous to the phenotypic plasticity seen in their hosts. This flexibility may be advantageous for the association's fitness, enabling *Ridgeia* and its symbionts to colonize and thrive in a broad range of habitats in this physiologically challenging environment.

Acknowledgements

This material is based upon work supported by the National Science Foundation under Grant No. DEB-1136484 to P.R. Girguis and OCE-1061934 to P.R. Girguis, and by NASA under grant # NNX09AB78G to P.R. Girguis. Li Liao was supported by a graduate fellowship awarded to her by the China Scholarship Council (CSC). We would like to thank the crews of the *RV Atlantis* and the *DSV Alvin*, as well as the *RV Western Flyer* and *ROV Doc Ricketts* for sampling. Special thanks to Prof. Dr. Moritz Lehmann at the University of Basel, Switzerland, for his very generous assistance with the isotope analyses. Thanks also to Charles Vidoudez and Heather Olins for assistance with sampling vent worms during these expeditions.

References

Andersen CL, Jensen JL, Ørntoft TF (2004) Normalization of real-time quantitative reverse transcription-PCR data: a model-based variance estimation approach to identify genes suited for normalization, applied to bladder and colon cancer data sets. *Cancer Research*, **64**, 5245–5250.

Andersen A, Flores J, Hourdez S (2006) Comparative branchial plume biometry between two extreme ecotypes of the hydrothermal vent tubeworm *Ridgeia piscesae*. *Canadian Journal of Zoology*, **84**, 1810–1822.

Black M, Lutz R, Vrijenhoek R (1994) Gene flow among vestimentiferan tube worm (Riftia pachyptila) populations from hydrothermal vents of the eastern Pacific. *Marine Biology*, **120**, 33–39.

Black M, Halanych K, Maas P *et al.* (1997) Molecular systematics of vestimentiferan tubeworms from hydrothermal vents and cold-water seeps. *Marine Biology*, **130**, 141–149.

Black MB, Trivedi A, Maas PA, Lutz RA, Vrijenhoek RC (1998) Population genetics and biogeography of vestimentiferan tube worms. *Deep-Sea Research Part II*, **45**, 365–382.

Bourbonnais A, Lehmann MF, Butterfield DA, Juniper SK (2012) Subseafloor nitrogen transformations in diffuse hydrothermal vent fluids of the Juan de Fuca Ridge evidenced by the isotopic composition of nitrate and ammonium. *Geochemistry, Geophysics, Geosystems*, **13**.

Carney SL, Flores JF, Orobona KM, Butterfield DA, Fisher CR, Schaeffer SW (2007) Environmental differences in hemoglobin gene expression in the hydrothermal vent tubeworm, *Ridgeia piscesae*. *Comparative Biochemistry and Physiology Part B: Biochemistry and Molecular Biology*, **146**, 326–337.

Cavanaugh CM, Gardiner SL, Jones ML, Jannasch HW, Waterbury JB (1981) Prokaryotic cells in the hydrothermal vent tube worm *Riftia pachyptila* Jones: possible chemoautotrophic symbionts. *Science*, **213**, 340–342.

Charlou J, Donval J, Douville E *et al.* (2000) Compared geochemical signatures and the evolution of Menez Gwen (37 50′N) and Lucky Strike (37 17′N) hydrothermal fluids, south of the Azores Triple Junction on the Mid-Atlantic Ridge. *Chemical Geology*, **171**, 49–75.

Childress J, Fisher C, Favuzzi J, Kochevar R, Sanders N, Alayse A (1991) Sulphide-driven autotrophic balance in the bacterial symbiont-containing hydrothermal vent tubeworm, *Riftia pachyptila* Jones. *The Biological Bulletin*, **180**, 135–153.

Cifuentes LA, Fogel ML, Pennock JR, Sharp JH (1989) Biogeochemical factors that influence the stable nitrogen isotope ratio of dissolved ammonium in the Delaware Estuary. *Geochimica et Cosmochimica Acta*, **53**, 2713–2721.

De Cian M, Regnault M, Lallier FH (2000) Nitrogen metabolites and related enzymatic activities in the body fluids and tissues of the hydrothermal vent tubeworm Riftia pachyptila. *Journal of Experimental Biology*, **203**, 2907–2920.

Di Meo CA, Wilbur AE, Holben WE, Feldman RA, Vrijenhoek RC, Cary SC (2000) Genetic variation among endosymbionts of widely distributed vestimentiferan tubeworms. *Applied and Environmental Microbiology*, **66**, 651–658.

Ding K, Seyfried WE Jr, Tivey MK, Bradley AM (2001) In situ measurement of dissolved H2 and H2S in high-temperature hydrothermal vent fluids at the main endeavour field, Juan de Fuca Ridge. *Earth and Planetary Science Letters*, 2001, **186**, 417–425.

Felbeck H, Jarchow J (1998) Carbon release from purified chemoautotrophic bacterial symbionts of the hydrothermal vent tubeworm *Riftia pachyptila*. *Physiological and Biochemical Zoology*, **71**, 294–302.

Felbeck H, Childress JJ, Somero GN (1981). Calvin-Benson cycle and sulphide oxidation enzymes in animals from sulphide-rich habitats.

Feldman R, Black M, Cary C, Lutz R, Vrijenhoek R (1997) Molecular phylogenetics of bacterial endosymbionts and their vestimentiferan hosts. *Molecular marine Biology and Biotechnology*, **6**, 268.

Fiala-Médioni A, Alayse A, Cahet G (1986) Evidence of in situ uptake and incorporation of bicarbonate and amino acids by a hydrothermal vent mussel. *Journal of Experimental Marine Biology and Ecology*, **96**, 191–198.

Fisher C, Childress J (1986) Translocation of fixed carbon from symbiotic bacteria to host tissues in the gutless bivalve *Solemya reidi*. *Marine Biology*, **93**, 59–68.

Gardebrecht A, Markert S, Sievert SM *et al.* (2011) Physiological homogeneity among the endosymbionts of *Riftia pachyptila* and *Tevnia jerichonana* revealed by proteogenomics. *The ISME Journal*, **6**, 766–776.

Gibson R, Atkinson R, Gordon J (2010) The biology of vestimentiferan tubeworms. *Oceanography and Marine Biology: An Annual Review*, **48**, 213–266.

Girguis PR, Childress JJ (2006) Metabolite uptake, stoichiometry and chemoautotrophic function of the hydrothermal vent tubeworm *Riftia pachyptila*: responses to environmental variations in substrate concentrations and temperature. *Journal of Experimental Biology*, **209**, 3516–3528.

Girguis PR, Lee RW, Desaulniers N *et al.* (2000) Fate of Nitrate Acquired by the Tubeworm *Riftia pachyptila*. *Applied and Environmental Microbiology*, **66**, 2783–2790.

Goffredi S, Childress J, Desaulniers N, Lee R, Lallier F, Hammond D (1997) Inorganic carbon acquisition by the hydrothermal vent tubeworm *Riftia pachyptila* depends upon high external pCO2 and upon proton-equivalent ion transport by the worm. *Journal of Experimental Biology*, **200**, 883–896.

Granger J, Sigman D, Rohde M, Maldonado M, Tortell P (2010) N and O isotope effects during nitrate assimilation by unicellular prokaryotic and eukaryotic plankton cultures. *Geochimica et Cosmochimica Acta*, **74**, 1030–1040.

Hahlbeck E, Pospesel MA, Zal F, Childress JJ, Felbeck H (2005) Proposed nitrate binding by hemoglobin in *Riftia pachyptila* blood. *Deep Sea Research Part I: Oceanographic Research Papers*, **52**, 1885–1895.

Harmer TL, Rotjan RD, Nussbaumer AD *et al.* (2008) Free-living tube worm endosymbionts found at deep-sea vents. *Applied and Environmental Microbiology*, **74**, 3895–3898.

Hentschel U, Felbeck H (1993). Nitrate respiration in the hydrothermal vent tubeworm Riftia pachyptila.

Hoch MP, Fogel ML, Kirchman DL (1992) Isotope fractionation associated with ammonium uptake by a marine bacterium. *Limnology and Oceanography*, **37**, 1447–1459.

Johnson KS, Childress JJ, Hessler RR, Sakamoto-Arnold CM, Beehler CL (1988) Chemical and biological interactions in the Rose Garden hydrothermal vent field, Galapagos spreading center. *Deep-Sea Research. Part A, Oceanographic Research Papers*, **35**, 1723–1744.

Jones ML (1985) On the Vestimentifera, new phylum: six new species, and other taxa, from hydrothermal vents and elsewhere. *Bulletin of the Biological Society of Washington*, **6**, 117–158.

Karl DM, Taylor GT, Novitsky JA *et al.* (1988) A microbiological study of Guaymas Basin high temperature hydrothermal vents. *Deep-Sea Research. Part A, Oceanographic Research Papers*, **35**, 777–791.

Kraft B, Strous M, Tegetmeyer HE (2011) Microbial nitrate respiration–genes, enzymes and environmental distribution. *Journal of Biotechnology*, **155**, 104–117.

Lee RW, Childress JJ (1994) Assimilation of inorganic nitrogen by marine invertebrates and their chemoautotrophic and methanotrophic symbionts. *Applied and Environmental Microbiology*, **60**, 1852–1858.

Lee RW, Robinson JJ, Cavanaugh CM (1999) Pathways of inorganic nitrogen assimilation in chemoautotrophic bacteria-marine invertebrate symbioses: expression of host and symbiont glutamine synthetase. *Journal of Experimental Biology*, **202**, 289–300.

Lilley M, Butterfield D, Olson E, Lupton J, Macko S, McDuff R (1993) Anomalous CH_4 and NH_4^+ concentrations at an unsedimented mid-ocean-ridge hydrothermal system. *Nature*, **364**, 45–47.

Markert S, Arndt C, Felbeck H *et al.* (2007) Physiological proteomics of the uncultured endosymbiont of *Riftia pachyptila*. *Science*, **315**, 247–250.

Markert S, Gardebrecht A, Felbeck H *et al.* (2011) *Status quo* in physiological proteomics of the uncultured *Riftia pachyptila* endosymbiont. *Proteomics*, **11**, 3106–3117.

McMullin ER, Hourdez S, Schaeffer SW, Fisher CR (2003) Phylogeny and biogeography of deep sea vestimentiferan tubeworms and their bacterial symbionts. *Symbiosis*, **34**, 1–41.

Minic Z, Hervé G (2003) Arginine metabolism in the deep sea tube worm Riftia pachyptila and its bacterial endosymbiont. *Journal of Biological Chemistry*, **278**, 40527–40533.

Minic Z, Simon V, Penverne B, Gaill F, Hervé G (2001) Contribution of the bacterial endosymbiont to the biosynthesis of pyrimidine nucleotides in the deep-sea tube worm *Riftia pachyptila*. *Journal of Biological Chemistry*, **276**, 23777–23784.

Montoya JP, McCarthy JJ (1995) Isotopic fractionation during nitrate uptake by phytoplankton grown in continuous culture. *Journal of Plankton Research*, **17**, 439–464.

Montoya J, Korrigan S, McCarthy J (1991) Rapid, storm-induced changes in the natural abundance of ^{15}N in a planktonic ecosystem, Chesapeake Bay, USA. *Geochimica et Cosmochimica Acta*, **55**, 3627–3638.

Moreno-Vivián C, Cabello P, Martínez-Luque M, Blasco R, Castillo F (1999) Prokaryotic nitrate reduction: molecular properties and functional distinction among bacterial nitrate reductases. *Journal of Bacteriology*, **181**, 6573–6584.

Nakhoul NL, Abdulnour-Nakhoul SM, Schmidt E, Doetjes R, Rabon E, Hamm LL (2010) pH sensitivity of ammonium transport by Rhbg. *American Journal of Physiology – Cell Physiology*, **299**, C1386–C1397.

Needoba JA, Harrison PJ (2004) Influence of low light and a light: dark cycle on NO_3 uptake, intracellular NO_3, and nitrogen isotope fractionation by marine phytoplankton. *Journal of Phycology*, **40**, 505–516.

Nyholm SV, Robidart J, Girguis PR (2008) Coupling metabolite flux to transcriptomics: insights into the molecular mechanisms underlying primary productivity by the hydrothermal vent tubeworm *Ridgeia piscesae*. *The Biological Bulletin*, **214**, 255–265.

Nyholm SV, Song P, Dang J, Bunce C, Girguis PR (2012) Expression and Putative Function of Innate Immunity Genes under in situ Conditions in the Symbiotic Hydrothermal Vent Tubeworm *Ridgeia piscesae*. *PLoS ONE*, **7**, e38267.

Pospesel MA, Hentschel U, Felbeck H (1998) Determination of nitrate in the blood of the hydrothermal vent tubeworm *Riftia pachyptila* using a bacterial nitrate reduction assay. *Deep-Sea Research Part I*, **45**, 2189–2200.

Reitzer L (2003) Nitrogen assimilation and global regulation in *Escherichia coli*. *Annual Reviews in Microbiology*, **57**, 155–176.

Richardson D, Berks B, Russell D, Spiro S, Taylor C (2001) Functional, biochemical and genetic diversity of prokaryotic nitrate reductases. *Cellular and Molecular Life Sciences: CMLS*, **58**, 165–178.

Robidart JC, Bench SR, Feldman RA *et al.* (2008) Metabolic versatility of the *Riftia pachyptila* endosymbiont revealed through metagenomics. *Environmental Microbiology*, **10**, 727–737.

Robidart JC, Roque A, Song P, Girguis PR (2011) Linking hydrothermal geochemistry to organismal physiology: physiological versatility in *Riftia pachyptila* from sedimented and basalt-hosted vents. *PLoS ONE*, **6**, e21692.

Sanders JG, Beinart RA, Stewart FJ, Delong EF, Girguis PR (2013) Metatranscriptomics reveal differences in in situ energy and nitrogen metabolism among hydrothermal vent snail symbionts. *The ISME Journal*, **7**, 1556–1567.

Scott KM, Boller AJ, Dobrinski KP, Le Bris N (2012) Response of hydrothermal vent vestimentiferan *Riftia pachyptila* to differences in habitat chemistry. *Marine Biology*, **159**, 435–442.

Sigman D, Casciotti K, Andreani M, Barford C, Galanter M, Böhlke J (2001) A bacterial method for the nitrogen isotopic analysis of nitrate in seawater and freshwater. *Analytical Chemistry*, **73**, 4145–4153.

Simon J (2002) Enzymology and bioenergetics of respiratory nitrite ammonification. *FEMS Microbiology Reviews*, **26**, 285–309.

Southward EC, Tunnicliffe V, Black M (1995) Revision of the species of *Ridgeia* from northeast Pacific hydrothermal vents, with a redescription of *Ridgeia piscesae* Jones (Pogonophora: Obturata = Vestimentifera). *Canadian Journal of Zoology*, **73**, 282–295.

Stewart FJ, Cavanaugh CM (2006) Symbiosis of thioautotrophic bacteria with *Riftia pachyptila*. In: *Molecular Basis of Symbiosis*, pp. 197–225. Springer, Berlin, Heidelberg.

Urcuyo I, Massoth G, MacDonald I, Fisher C (1998) In situ growth of the vestimentiferan *Ridgeia piscesae* living in highly diffuse flow environments in the main Endeavour Segment of the Juan de Fuca Ridge. *Cahiers de Biologie Marine*, **39**, 267–270.

Urcuyo IA, Massoth GJ, Julian D, Fisher CR (2003) Habitat, growth and physiological ecology of a basaltic community of *Ridgeia piscesae* from the Juan de Fuca Ridge. *Deep Sea Research Part I: Oceanographic Research Papers*, **50**, 763–780.

Urcuyo IA, Bergquist DC, MacDonald IR, VanHorn M, Fisher CR (2007) Growth and longevity of the tubeworm *Ridgeia piscesae* in the variable diffuse flow habitats of the Juan de Fuca Ridge. *Marine Ecology Progress Series*, **344**, 143–157.

Vandesompele J, De Preter K, Pattyn F *et al.* (2002) Accurate normalization of real-time quantitative RT-PCR data by geometric averaging of multiple internal control genes. *Genome Biology*, **3**, research0034.

Von Damm KV, Edmond JT, Grant B (1985) Chemistry of submarine hydrothermal solutions at Guaymas Basin, Gulf of California. *Geochimica et Cosmochimica Acta*, **49**, 2221–2237.

Wada E (1980) Nitrogen isotope fractionation and its significance in biogeochemical processes occurring in marine environments. *Isotope Marine Chemistry*, **1**, 375–398.

Wada E, Hattori A (1978) Nitrogen isotope effects in the assimilation of inorganic nitrogenous compounds by marine diatoms. *Geomicrobiology Journal*, **1**, 85–101.

Wankel SD, Germanovich LN, Lilley MD *et al.* (2011) Influence of subsurface biosphere on geochemical fluxes from diffuse hydrothermal fluids. *Nature Geoscience*, **4**, 461–468.

Waser NA, Yin K, Yu Z *et al.* (1998) Nitrogen isotope fractionation during nitrate, ammonium and urea uptake by marine diatoms and coccolithophores under various conditions of N availability. *Marine Ecology Progress Series*, **169**, 29–41.

Experiments and assays were designed by L.L. Samples were collected by P.G. All molecular biological analyses were conducted by L.L. Isotope analyses were conducted by S.W., L.L. and P.G. wrote the manuscript, with significant contributions from S.W., C.C. and M.W.

Data accessibility

DNA sequences recovered during primer design: Dryad doi:10.5061/dryad.555hd.

Sample collection sites: locations and images of collections as listed in this manuscript may be found at http://4dgeo.whoi.edu/alvin.

Blood concentrations of nitrate and ammonium for each tested individual, qRT–PCR results, gene expression data and isotope data: Dryad doi:10.5061/dryad.555hd.